Materials and Methods

Reagents Anti-IFN-γ, anti-IL-12 and other mAbs (purified, biotinylated, or fluorophore-conjugated) were from BD Biosciences or Tonbo Biosciences (San Diego CA) unless otherwise indicated. 11B11 anti-IL-4 and recombinant human IL-2 were from the Biological Response Modifiers Program of the NCI (Frederick, MD). NP-BSA and NP-PSA (for capture in ELISA) as well as NP-OVA (for immunization) were obtained from Biosearch (Novato CA). Recombinant mouse IFN-γ, SRBC (sheep red blood cells), D-glucose, and 2-deoxyglucose were from Thermo Fisher Scientific (Waltham MA). Recombinant mouse IL-4 was from Peprotech (Rocky Hill NJ). IL-21 was from R&D Systems (Minneapolis, MN). Tamoxifen, 4-hydroxy-tamoxifen, and oligomycin were from Sigma-Aldrich Chemicals (St. Louis MO).

Mice and CD4 T cell transfer model All mice [C57BL/6-J; *Tcra -/-* ("TCRα KO"); *Rosa26*-CreER^{T2} *Hif1a*$^{fl/fl}$ ("HIF-1α cKO"), *Rosa26*-CreER^{T2} *Epas1*$^{fl/fl}$ ("HIF-2α cKO"), *Rosa26*-CreER^{T2} *Hif1a*$^{fl/fl}$ *Epas1*$^{fl/fl}$ (HIF-1α, HIF-2α double cKO), *Rosa26*-CreER^{T2} *Rptor*$^{fl/fl}$ (1) and *Rosa26*-CreER^{T2} controls; dLck-iCre, *Rictor* f/f ("Rictor cKO") and dLck-iCre controls (2), and Lck-IκBα-ΔN (3) transgenic mice were housed in ventilated micro-isolators under Specified Pathogen-Free conditions in a Vanderbilt mouse facility and used under protocols approved by the Institutional Animal Care and Use Commity. HIF-deficient (Δ/Δ) T cells were generated by three injections of tamoxifen as described previously (1). Balanced mixes of males and females were used at 6–8 wk of age following approved protocols. Healthy donor and recipient mice of appropriate genotype were selected randomly for experiments without size or gender preference. For cell transfer experiments, CD4$^+$ T cells were purified by depleting CD8$^+$ T cells and B cells using biotinylated anti-CD8 Ab and biotinylated anti-B220 Ab followed by streptavidin-conjugated microbeads (iMag^{TM}; BD Biosciences, San Jose CA). Pooled WT, *Hif1a*$^{Δ/Δ}$, *Epas1*$^{Δ/Δ}$, and *Hif1a*$^{Δ/Δ}$ *Epas1*$^{Δ/Δ}$, or IκBα-ΔN transgenic CD4$^+$ T cells (5×10^6 cells per recipient mouse)

were injected intravenously (i.v.) into *Tcra -/-* recipients followed by immunization and analysis.

Immunizations and measurements of Ab responses After collection of pre-immune sera, mice were immunized with SRBCs (2×10^8 cells per mouse) and analyzed 1 week after immunization as described (4). In some cases, mice were immunized with NP_{16}-ovalbumin (OVA) (100 μg intra-peritoneally, i.e., i.p.) in alum (Imject, Thermo Fisher Scientific, Waltham MA), boosted after three weeks, and analyzed one week thereafter, as described (4). Immune sera were collected and analyzed for Ag-specific isotype Ab using HRP-conjugated or biotinylated antibodies (Thermo Fisher) as described (4). To detect SRBC-specific Ab, an SRBC suspension ($5x10^6$ cells / 100 μl PBS) was added to each well of flat bottom 96-well ELISA plates and incubated overnight at 4^0 C. Without disturbing the cell layer, 20 μl of 1.8% glutaraldehyde solution was gently added followed by incubation (30 min; 20^0 C). The plates were washed 4 times with 200 μl of PBS, and non-specific binding sites were then blocked (1 hr) with 2% skim milk in PBS. Serial two-fold dilutions of sera (starting at 1:100) were added in duplicate followed by incubation for 2 hr at 37^0 C, washing (3x with 200 μl of PBS), and incubation with 100 μl biotinylated-secondary Ab (anti-mouse IgG1 or anti-mouse IgG2c (Southern Biotech) (1.5 hr; 20^0 C). After washing (3x with 200 μl of PBS), alkaline phosphatase-conjugated avidin was then added to the wells and incubated (1 hr; 20^0 C). After washing, alkaline phosphatase substrate pNPP (Sigma Aldrich) was added to each well and the plate incubated at 20^0 C and analyzed for absorbance at 405 nm. Relative levels of all- and high-affinity anti-NP antibodies were measured by capturing the hapten-binding Ab on plate-immobilized NP_{20}-BSA or NP_2-PSA, respectively. Data for Ag-specific Ab are shown after subtraction of low OD values from pre-immune controls analyzed together with the immune sera and were separately determined to match values yielded by titration.

Flow cytometry Flow cytometric phenotyping of in vivo immune responses were conducted 7 d after primary (SRBC) or booster (NP-ovalbumin) immunization as indicated. For detection of NP-specific germinal center responses, spleen or lymph node cells ($2x10^6$) were stained with GL7, anti-CD95, -CD38, -B220, NP-APC and a dump cocktail containing monoclonal antibodies for IgD, 7-AAD, CD11b, CD11c, F4/80, and Gr1. The flow cytometric strategy for analysis of Tfr and Tfr as published (7, 22). For these and other flow cytometric analyses, fluorescence emission data on cell suspensions were collected on BD flow cytometers (FACSCanto, LSR or Fortessa) driven by BD FACS Diva software, then processed using Flow-Jo software (FlowJo LLC, formerly TreeStar, Ashland OR). Fluorophore-conjugated and antibodies as well as fluorescence-labeled streptavidin for direct and indirect immune fluorescence staining of lymphoid suspensions are compiled in SI Appendix Table 1.

Measurements of RNA and proteins Viable $CD4^+$ $CD44^{hi}$ $CXCR5^-$ $PD1^-$ and $CD4^+$ $CD44^{hi}$ $CXCR5^+$ $PD1^+$ splenocytes were flow purified using a FACS Aria and deposited into Trizol reagent (Ambion) after staining suspensions of splenocytes from immunized mice (SRBC or NP-ovalbumin). Total RNA was isolated from biological replicates. After cDNA synthesis by reverse transcription, gene expression was analyzed in duplicate samples using SYBR green PCR master-mix (Applied Biosystems, Warrington, UK) by quantitative real-time RT-PCR (qRT^2-PCR). Data for each sample normalized to levels of internal control (HPRT) are presented as values further normalized to WT control and averaged across the PCR replicates. Primer pairs are detailed in Supplementary Table 2. To assay mTOR-dependence of HIF-1α and HIF-2α induction, purified $CD4^+$ T cells were activated with plate-bound anti-CD3 (2.5 μg/ml) and anti-CD28 (2.5 μg/ml). Proteins in whole cell extracts prepared 1 d after activation were resolved by SDS-PAGE, transferred onto polyvinylidene difluoride membranes (Millipore), and then incubated with rabbit antibodies against HIF-1α, HIF-2α (Novus Biological, Littleton, CO), or goat anti-actin (Santa Cruz) Abs followed by rinsing and application of the appropriate fluorophore-conjugated, species-specific secondary anti-Ig antibodies (Rockland

Immunochemicals or LI-COR). Proteins were visualized and quantitated by laser excitation and infrared imaging (Odyssey, LI-COR).

Th cell differentiation and analysis $CD4^+$ T cells were purified (≥95%) using anti-CD4 microbeads (Miltyeni, Auburn CA) after CreERT2 induction in vivo by tamoxifen injections as described above, and then activated with plate-bound anti-CD3 plus soluble anti-CD28 (2.5 μg/ml each). Cells were then cultured (5 d) in equal portions in T helper subset differentiating conditions [Th1, anti-IL-4 (5 μg/ml) and IL-12 (10 ng/ml); Th2, anti-IL-12 (3 μg/ml), anti-IFN-γ (3 μg/ml), and IL-4 (10 ng/ml)], each in the presence of 4-hydroxytamoxifen (50 ng/ml) with addition of fresh rhu-IL-2 every other day as described (2), of which one portion of each helper condition was maintained at 1% pO_2 throughout. One day prior to secondary stimulation, one set of cells was transferred from 21% to 1% pO_2. Cells were re-stimulated with PMA (50 nM) and ionomycin (1 μg/ml) for 6 h for intracellular staining. For cytokine measurement in culture supernatant, cells were re-stimulated with plate-bound anti-CD3 plus soluble anti-CD28 (0.5 μg/ml each) and either stained for intracellular IFN-γ and IL-4 along with surface CD4, as described (2). Cytokine concentrations in culture supernatants were measured using a multiplex Th1/2/17 Cytokine Bead Array (BD Bioscience). To measure frequencies of cytokine-producing Tfh cells, splenocyte suspensions prepared from SRBC-immunized mice (7 d) were first stained for CD4, CD44, CXCR5, and PD1, then re-stimulated for 3 hr with PMA (50 ng/ml) plus ionomycin (1 μg/ml) with the addition of Golgi-Stop. Surface-stained restimulated cells were then fixed and permeabilized with Flow Cytometry Fix/Perm buffer solutions (Tonbo Bioscience) followed by intracellular staining for retained cytokine.

Seahorse assays Purified $CD4^+$ cells were cultured (2 d, 37°C) at pO_2 of 21% (normoxia) or 1% (hypoxia) after activation with anti-CD3 and soluble anti-CD28 as for T helper differentiation. The cells were then washed, rested for 3 h, and further cultured for 20 h in normoxia or hypoxia in the presence or absence of anti-CD3 (0.5 μ g/ml), IL-2 (20 U/ml), IL-6 (20 ng/ml), or IL-21 (100 ng/ml). Extracellular Acidification Rate (ECAR) and Oxygen

Consumption Rate (OCR) were measured using Seahorse XF96 extracellular flux analyzer (Agilent Technology, Santa Clara, CA) as described (4). Briefly, cultured $CD4^+$ T cells were washed twice, resuspended in XF Base Media (Agilent Technologies) supplemented with 2 mM L-glutamine, and equal numbers of CD4 T cells (1.5×10^5) were plated on extracellular flux assay plates (Agilent Technologies) coated with 2.5 μg/ml CellTak (Corning) according to the manufacturer's protocol. Before extracellular flux analysis, CD4 T cells were rested (25 minutes at 37°C, atmospheric CO_2) in XF Base Media. OCR and ECAR were measured before and after the sequential addition of 10 mM D-glucose, 1 μM oligomycin, and 50 mM 2-deoxyglucose.

Statistical analysis The primary analyses were conducted on pooled data points from independent samples and replicate experiments, using an unpaired two-tailed Student's *t* test with post-test validation of its suitability. In certain instances, unpaired testing with Welch's correction was used as indicated. Two-way ANOVA with Bonferroni correction for multiple comparisons was used for statistical analysis across ELISA titration curves to compare wild-type to each mutant samples set, followed by a secondary comparison at set dilutions using the *t* test. Data are displayed as mean (± SEM), and results were considered "statistically significant" when the p value of for the null hypothesis of a comparison was <0.05, i.e. two standard deviations from mean.

References

1. Raybuck AL, *et al.* (2018) B Cell-Intrinsic mTORC1 Promotes Germinal Center-Defining Transcription Factor Gene Expression, Somatic Hypermutation, and Memory B Cell Generation in Humoral Immunity. *J Immunol* 200(8):2627-2639.
2. Lee K, *et al.* (2010) Mammalian target of rapamycin protein complex 2 regulates differentiation of Th1 and Th2 cell subsets via distinct signaling pathways. *Immunity* 32(6):743-753.
3. Aronica MA, *et al.* (1999) Preferential role for NF-kappa B/Rel signaling in the type 1 but not type 2 T cell-dependent immune response in vivo. *J Immunol* 163(9):5116-5124.
4. Cho SH, *et al.* (2016) Germinal centre hypoxia and regulation of antibody qualities by a hypoxia response system. *Nature* 537(7619):234-238.

Supplemental Figure 1. HIF induction in Tfh and activated CD4$^+$ Tcells, and impact of its loss from mature hematopoietic cells. (A) Flow cytometric results from intracellular staining for HIF-1α in the gate for Tfh versus CD44^{hi} PD-1^{neg} CXCR5 ^{neg} event, or IgG negative control, using biologically independent cohorts of mice immunized as in Fig. 1D, and showing only WT CD4$^+$ T cells. One experiment's result from among three replicates is shown (left). Bar graph to the right shows mean (±SEM) specific level of HIF-1α in the indicated populations after subtraction of non-specific signal (IgG1 control) and normalization to the specific signal for the PD-1^{neg} CXCR5^{neg} CD44^{hi} CD4$^+$ cells in each of the 3 independent experiments. (B) mTOR regulates HIF-1a expression in Tfh cells. As in Fig. 1E, PD1$^+$ CXCR5$^+$ CD4$^+$ Tfh cells (WT, *Rptor*$^{Δ/Δ}$, or *Rictor*$^{Δ/Δ}$ as indicated) were subjected to intracellular staining for HIF-1α. The bar graph shows mean (±SEM) specific level of HIF-1α [normalized to the WT sample (=1) in each experiment of the 3 replications. (C) Seahorse metabolic flux results from the experiments in Fig. 1F, using control samples cultured at 21% pO_2 without TCR restimulation. Display is as in Fig. 1F; * indicates $p<0.05$ between WT and single or doubly HIF-deficient CD4$^+$ T cells. "+" indicates $p\leq0.05$ in comparing *Hif1a*$^{Δ/Δ}$ (red) and *Hif1a*$^{Δ/Δ}$*;Epas1*$^{Δ/Δ}$ (purple) CD4$^+$ T cells. (D, E) *Rosa26*-CreER^{T2}; *Hif1a*$^{f/f}$, *Rosa26*-CreER^{T2}; or *Hif1a*$^{f/f}$; *Epas1*$^{f/f}$, *Rosa26*-CreER^{T2} mice were injected with tamoxifen (TMX) and immunized with NP-OVA as in Fig 2. Shown are the numbers and frequencies of B220$^+$ B cells (D) and CD4$^+$ T cells (E) in spleens at the time of harvest. Bar graphs display mean (±SEM) from 3 independent experiments (n= 9 WT vs 3 HIF-1α cKO vs 5 HIF-1α; HIF-2α double cKO mice). (F) HIF regulates germinal center response. *Rosa26*-CreER^{T2}; or *Hif1a*$^{f/f}$; *Epas1*$^{f/f}$, *Rosa26*-CreER^{T2} mice were injected with tamoxifen (TMX) and immunized with SRBC. Size of GL7-positive GC region (upper panel), and intensity of GL7 (lower panel) in GC were quantitated using Image J software. Three splenic regions per mouse for each of the mice. Bar graph shows mean (±SEM) from the biologically independent replicates (6 WT vs 5 HIF dKO, divided equally between two separate batches of mice injected with tamoxifen followed by immunization).

Supplemental Figure 2. HIF regulates Ag-specific Ab production. Using sera analyzed in Fig 2D, all-affinity (anti-NP_{20}) and high-affinity (anti-NP_2) IgG1 (A) and IgG2c (B) in sera of immunized and boosted mice that were either WT or HIF-deficient as indicated. Shown are the mean (±SEM) values across serial 2-fold dilutions. Assessment of the null hypothesis was conducted as in the Methods, with the p values shown for each of two dilutions in the linear range based on unpaired t test.

Supplemental Figure 3. Frequencies, numbers, and properties of B and CD4$^+$ T cells in *Tcra* -/- recipients after adoptive transfer of WT of HIF-deficient CD4$^+$ T cells. As in Fig 3,

HIF sufficient and deficient CD4 T cells were isolated after three sequential tamoxifen injections of donor mice (*Rosa26*-CreER^{T2}, *Hif1a*$^{f/f}$; *Hif1a*$^{f/f}$, *Epas1*$^{f/f}$ *Rosa26*-CreER^{T2}, or *Rosa26*-CreER^{T2} controls) and adoptively transferred into T cell-deficient *Tcra* -/- (TCRα KO) recipient mice. (A) Frequencies of Treg in donor CD4^{+} T cells were analyzed prior to adoptive transfer. Shown are one representative experiment's sample set in the viable CD4^{+} gate, with the mean (±SEM) of the samples of three biological replicate experiments. (B, C) Frequencies and numbers of B220^{+} B cells (B) and CD4^{+} T cells (C) in spleen were analyzed at 7 days after SRBC immunization. None of these differences were "statistically significant". (D) HIF-1 modulates Bcl6 but not ICOS expression in Tfh-phenotype cells. Representative histograms of ICOS and Bcl6 in the PD1^{+} CXCR5^{+} CD4^{+} CD44^{hi} (Tfh) gate. Inset numbers display the mean (±SEM) geometric MFI values collected for all six samples for each genotype. Bar graphs show the mean (±SEM) Tfh-specific increases in geometric MFI (gMFI) for ICOS and Bcl-6 in two independent experiments, after subtraction of the non-Tfh MFI. Total of six recipient mice for each genotype of T cells; differences for Bcl6 (WT vs HIF-deficient) also were statistically significant for total MFI values inset into the histograms.

Supplemental Figure 4. CD4^{+} T cell-intrinsic mTORC2 regulates the balance between follicular regulators and Tfh cells. (A, B) T cell-specific Rictor-deficient mice [*Rictor*$^{f/f}$; *dLck*-iCre (28)] were immunized with SRBC and analyzed 1 wk thereafter. Shown are representative flow plots (A) and the mean (±SEM) values (B) of frequencies and numbers of GC B cells (GL7^{+} CD95^{+} GC-phenotype B cells in IgD^{neg} B220^{+}-gated splenocytes) in three independent experiments. (C) Representative flow plot of FoxP3 intracellular staining in the PD1^{+} CXCR5^{+} CD4^{+} CD44^{hi} (Tfh) gate. (D) Frequencies of FoxP3^{neg} PD1^{+} CXCR5^{+} CD4^{+} CD44^{hi} Tfh cells (left) and FoxP3^{+} CD4^{+} PD1^{+} CXCR5^{+} CD4^{+} CD44^{hi} cells. (E) Ratio of Tfr to Tfh frequencies in PD1^{+} CXCR5^{+} CD4^{+} CD44^{hi} cells in spleen from three independent experiments. (F) Levels of mRNA encoded by the *Il21, Bcl6, Prdm1, and Foxp3* genes were measured by qPCR after reverse transcription of total RNA from flow cytometrically purified Tfh cells from *Rictor*$^{f/f}$; *dLcK*-iCre mice and WT controls) 1 week after SRBC-immunization. Bar graphs show mean (± SEM) expression (relative to HPRT in the sample) measured in three independent replicate preparations. For each panel, assessment of the null hypothesis was conducted as in the Methods, with the p values shown based on unpaired t tests.

Supplemental Figure 5. Normal Tfh cell differentiation despite global NF-κB blockade in CD4^{+} T cells. (A-D) CD4^{+} T cells [IκBα(ΔN) transgenic (47) and WT controls] were transferred into TCRα KO recipient mice that were then immunized with SRBC and analyzed after seven

days. Frequencies and numbers of (A) $CD4^+$ T cells, (B) $GL7^+$ $CD95^+$ IgD^{neg} GC-phenotype B cells, (C) $FoxP3^{neg}$ $PD1^+$ $CXCR5^+$ $CD4^+$ $CD44^{hi}$ Tfh cells, and (D) $FoxP3^+$ $CD4^+$ $PD1^+$ $CXCR5^+$ $CD4^+$ $CD44^{hi}$ Tfr cells among splenocytes. Bar graphs show mean (± SEM) values from two independent experiments (each with two recipients of each genotype). (E) Mean (±SEM) ratios of Tfr to Tfh cells in the spleens of immunized recipient mice. (F) Initial frequencies of Treg comparable prior to transfers of $CD4^+$ T cells. For each panel, assessment of the null hypothesis was conducted as in the Methods, with the p values shown based on unpaired t tests.

Supplemental Figure 6. HIF-1 suppresses IL-2-induced increase in respiration by activated $CD4^+$ T cells. (A, B) As in Fig. 5, $CD4^+$ T cells of the indicated genotypes were cultured (2 d) after activation with αCD3 and αCD28, then rinsed, replated in equal numbers, and further cultured for 20 hr with and without IL-2 or IL-21 at (A) pO_2 of 21% (normoxia) or (B) 1% (hypoxia). Equal numbers of viable $CD4^+$ T cells were then re-plated and assayed in a metabolic flux analyzer. Shown for each analysis point across the time course (1.2 hr in 6 min intervals, with injections after three samplings) are the mean (±SEM) data determined from four biologically independent experiments. * indicates $p<0.05$ between WT and single or doubly HIF-deficient $CD4^+$ T cells. (C) As in Fig. 5A, purified $CD4^+$ T cells (WT, *Hif1a*$^{\Delta/\Delta}$, and *Hif1a*$^{\Delta/\Delta}$*;Epas1*$^{\Delta/\Delta}$, as indicated) were cultured (2 d) after activation with αCD3 and αCD28, then rinsed, replated in equal numbers, and further cultured for 20 hr in the presence of IL-6 at pO_2 of 21% (normoxia) or 1% (hypoxia). Equal numbers of viable $CD4^+$ T cells were then re-plated and assayed in a metabolic flux analyzer as detailed in the *Methods*. Shown for each analysis point across the time course (1.2 hr in 6 min intervals, with injections after three samplings) are the mean (±SEM) data determined from three biologically independent experiments. (D) IL-21 regulates the expression of IL-21R in $CD4^+$ T cells. $CD4^+$ T cells were cultured (2 d) after activation with αCD3 and αCD28, then rinsed, replated in equal numbers, and further cultured for 20 hr with and without IL-2 or IL-21. The cells were then analyzed by qPCR of their total RNA. Signals for *Il21r* (IL-21 receptor) were first normalized to HPRT, and values for the activated samples in an experiment were then expressed relative to measurements for WT $CD4^+$ T cells without any cytokine (set as relative level of 1). Shown are the mean (±SEM) values for *Il21r* for each genotype from three independent replicate samples.

Supplemental Figure 7. Lower 2NBDG uptake by Tfh cells despite higher uptake by GC B cells compared to the non-follicular populations. Glucose uptake was measured by the fluorescent, non-metabolized glucose analogue 2-NBDG (2-(N-(7-Nitrobenz-2-oxa-1,3-diazol-4-yl)Amino)-2-Deoxyglucose) (ThermoFisher). At 1 wk after immunization with SRBC, mice were fasted for 6 hr, injected with 2-NBDG (5 mM, 200 μl/mouse *i.p.*), and harvested 30 minutes later. Shown are representative flow plots of the glucose uptake signal in (A) GC-phenotype

($GL7^{+}$ $CD95^{+}$) B cells and non-GC ($GL7^{neg}$ $CD95^{neg}$) splenic B cells, and (B) Tfh ($CD44^{hi}$ PD-1^{+} $CXCR5^{+}$), and $CD44^{hi}$ PD-1^{neg} $CXCR5^{neg}$ CD4 T cells. Inset numbers in black font represent the % 2-$NBDG^{hi}$ cells of the indicated subset, while those in blue font are mean (±SEM) MFI from three independent replicate preparations.

Supplemental Figure 8. $CD4^{+}$ T cell differentiation to IL4 and IFN-γ production is hypoxia- and HIF-independent. As in Fig. 6, $CD4^{+}$ T cells were activated and differentiated into Th1 and Th2 cells at pO_2 of 21% (normoxia) or pO_2 of 1% (hypoxia). Viable cells were re-stimulated with PMA and ionomycin, and frequencies of IFN-γ (in Th1 condition) and IL-4 (in Th2 condition) were measured by intracellular staining. Bar graphs show mean (± SEM) cytokine positive cells among $CD4^{+}$ cells from replicates in three independent experiments. None of the differences were significant in statistical testing.

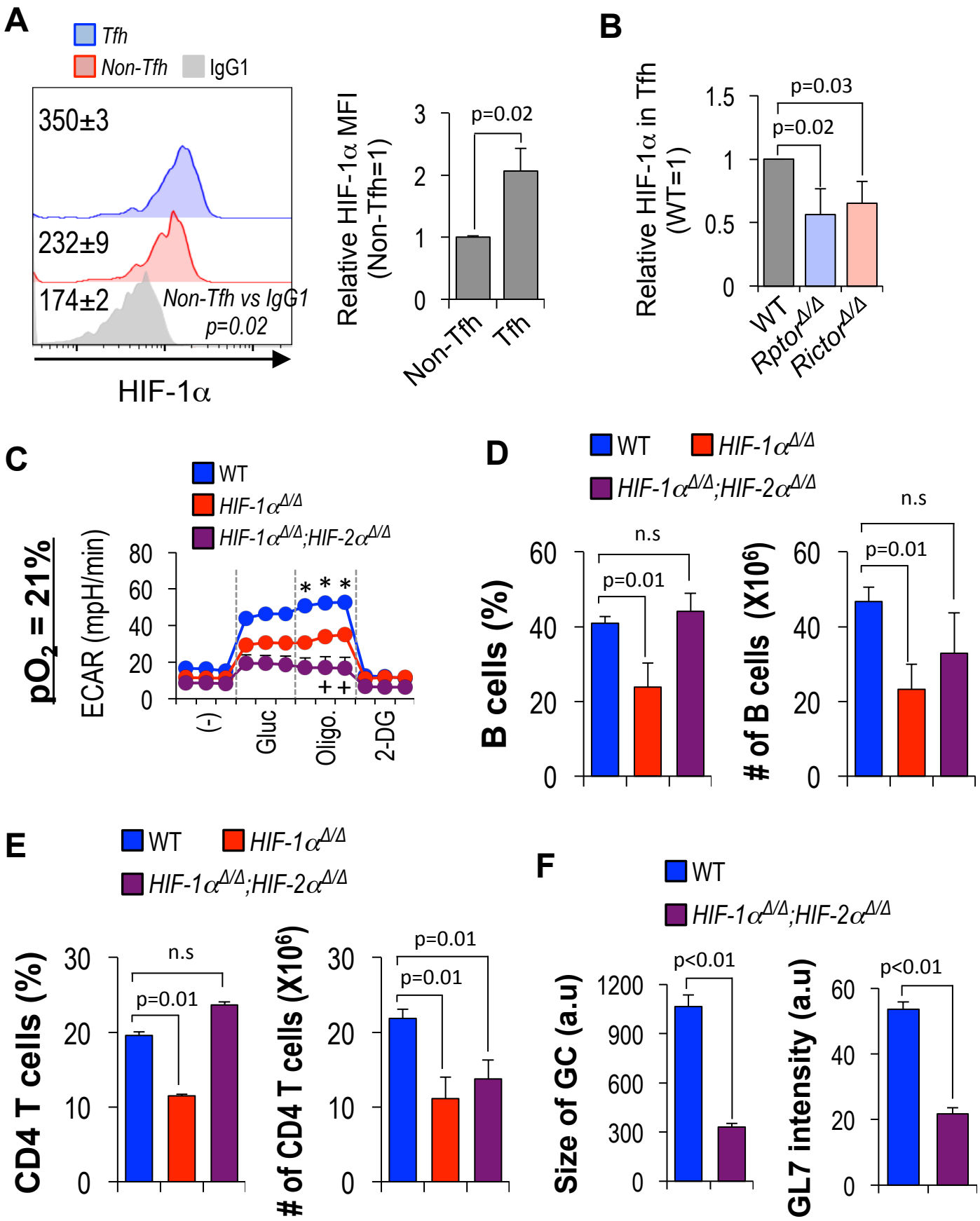

Supplemental Fig. 1

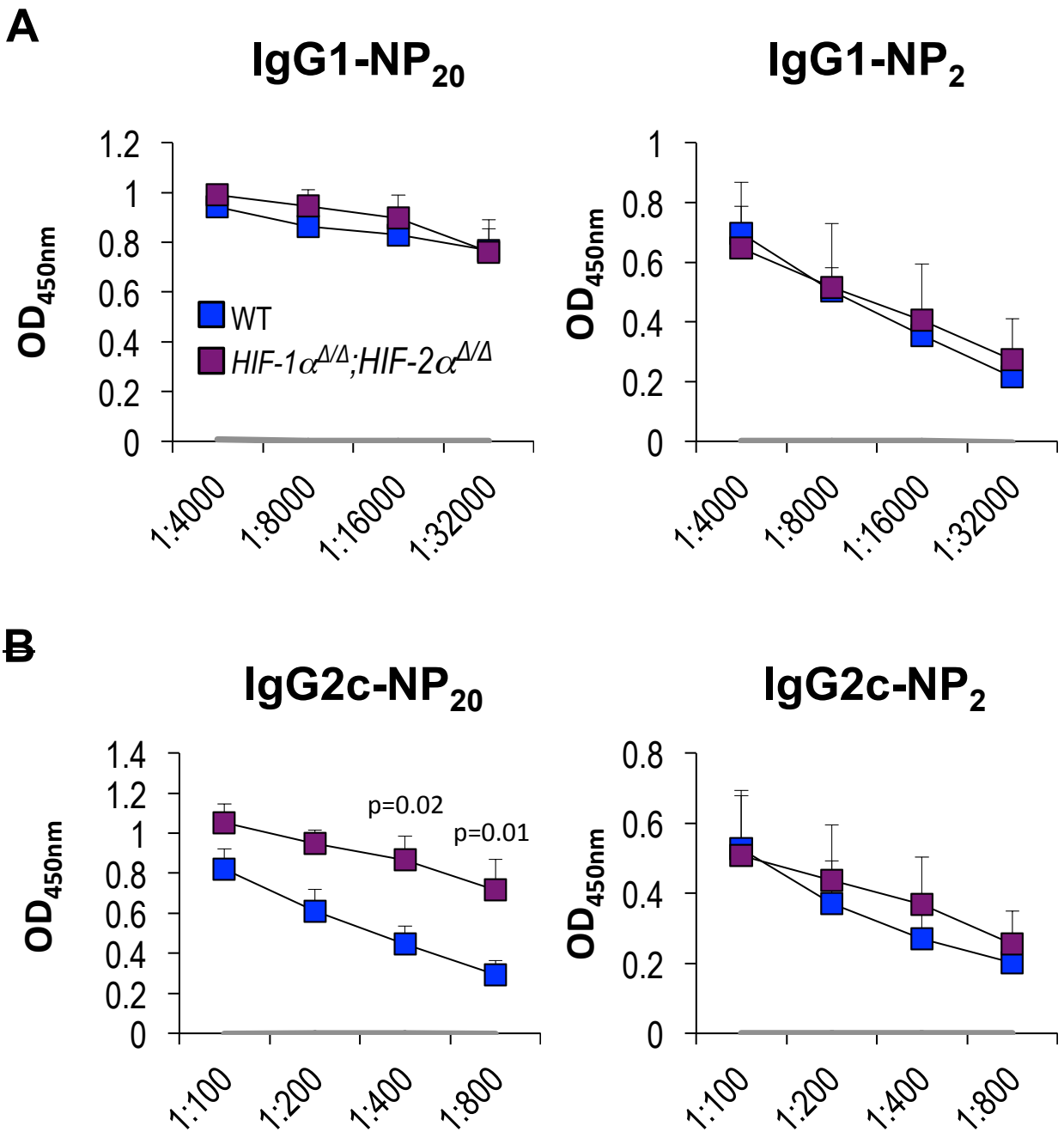

Supplemental Fig. 2

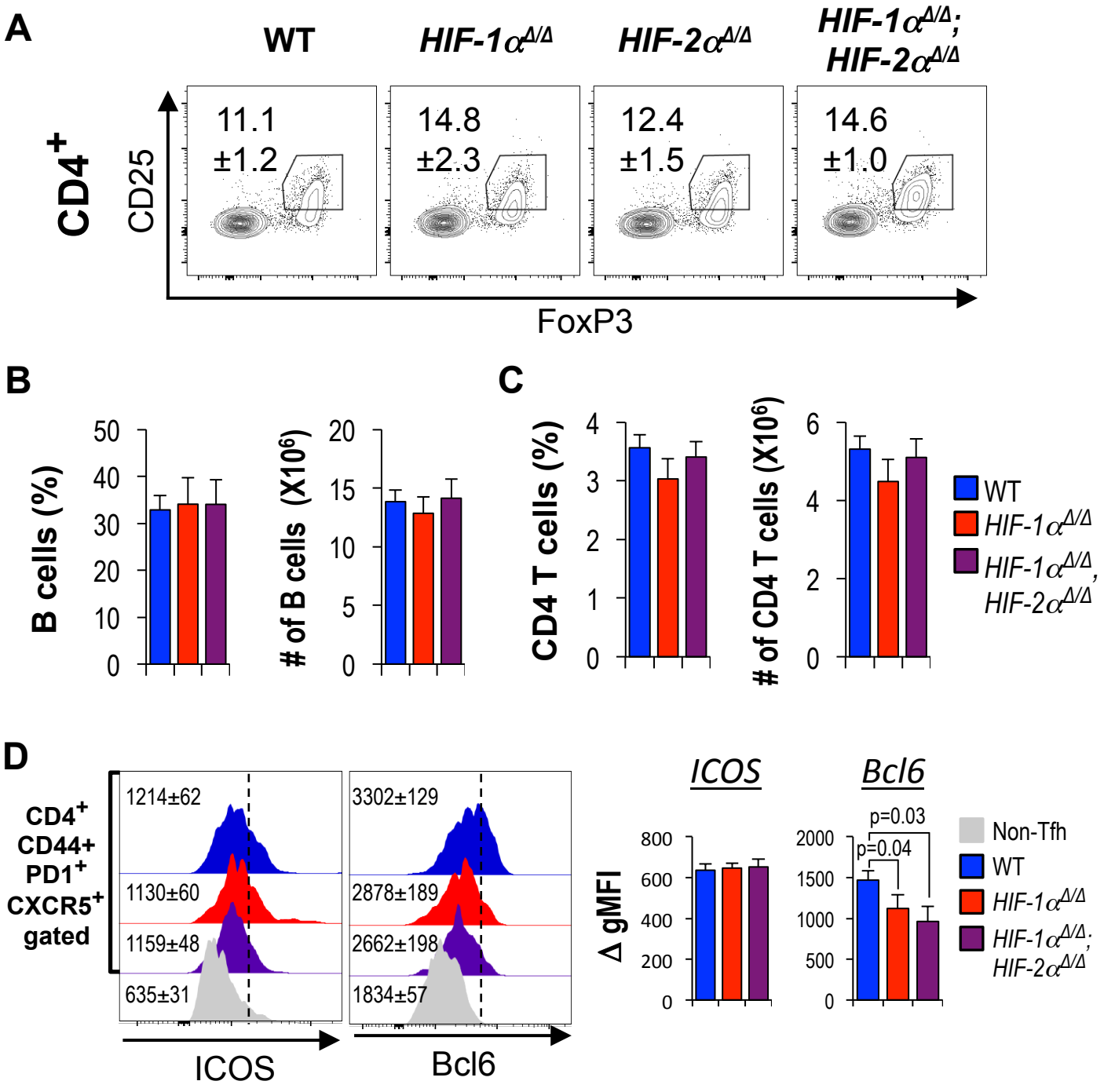

Supplemental Fig. 3

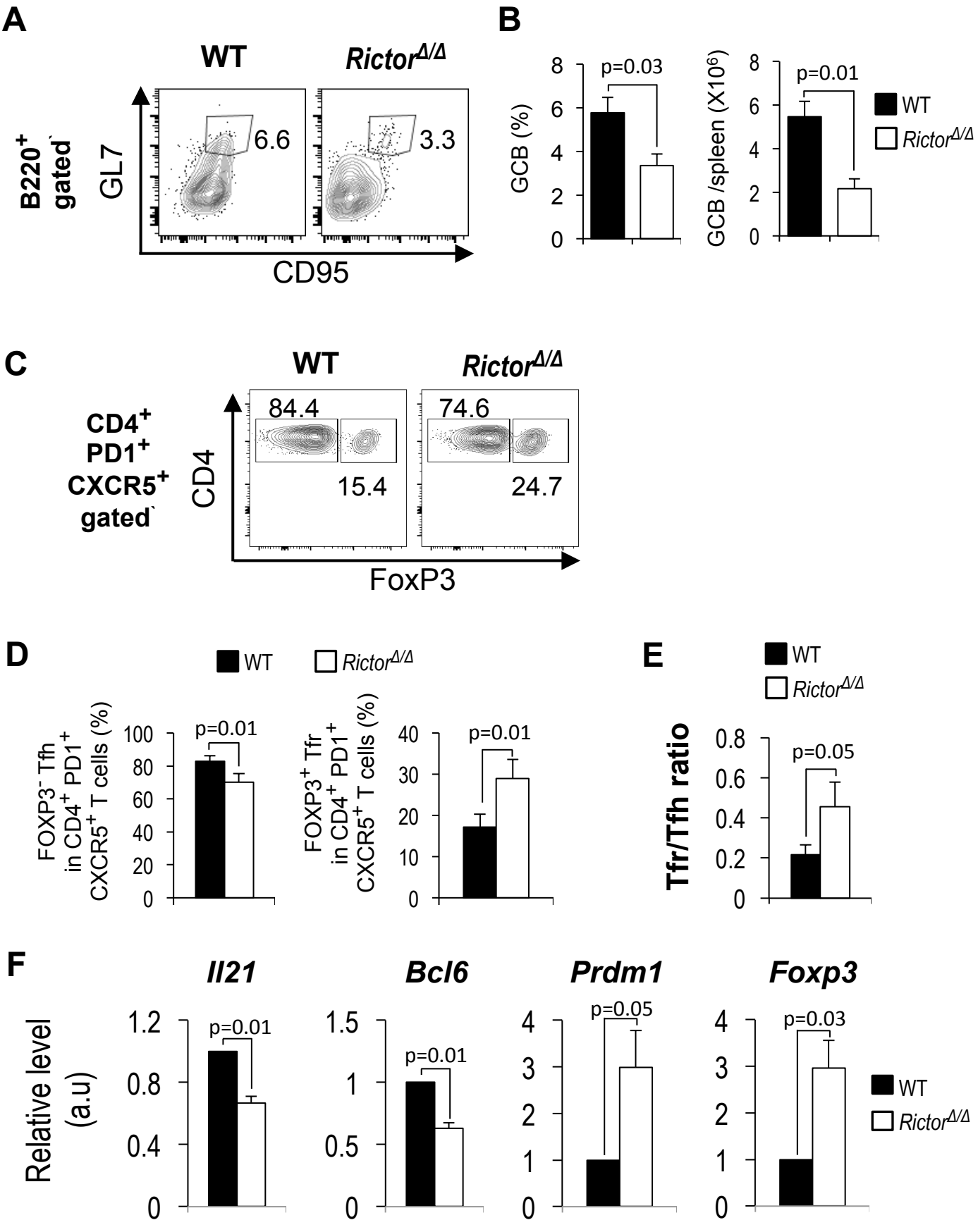

Supplemental Fig. 4

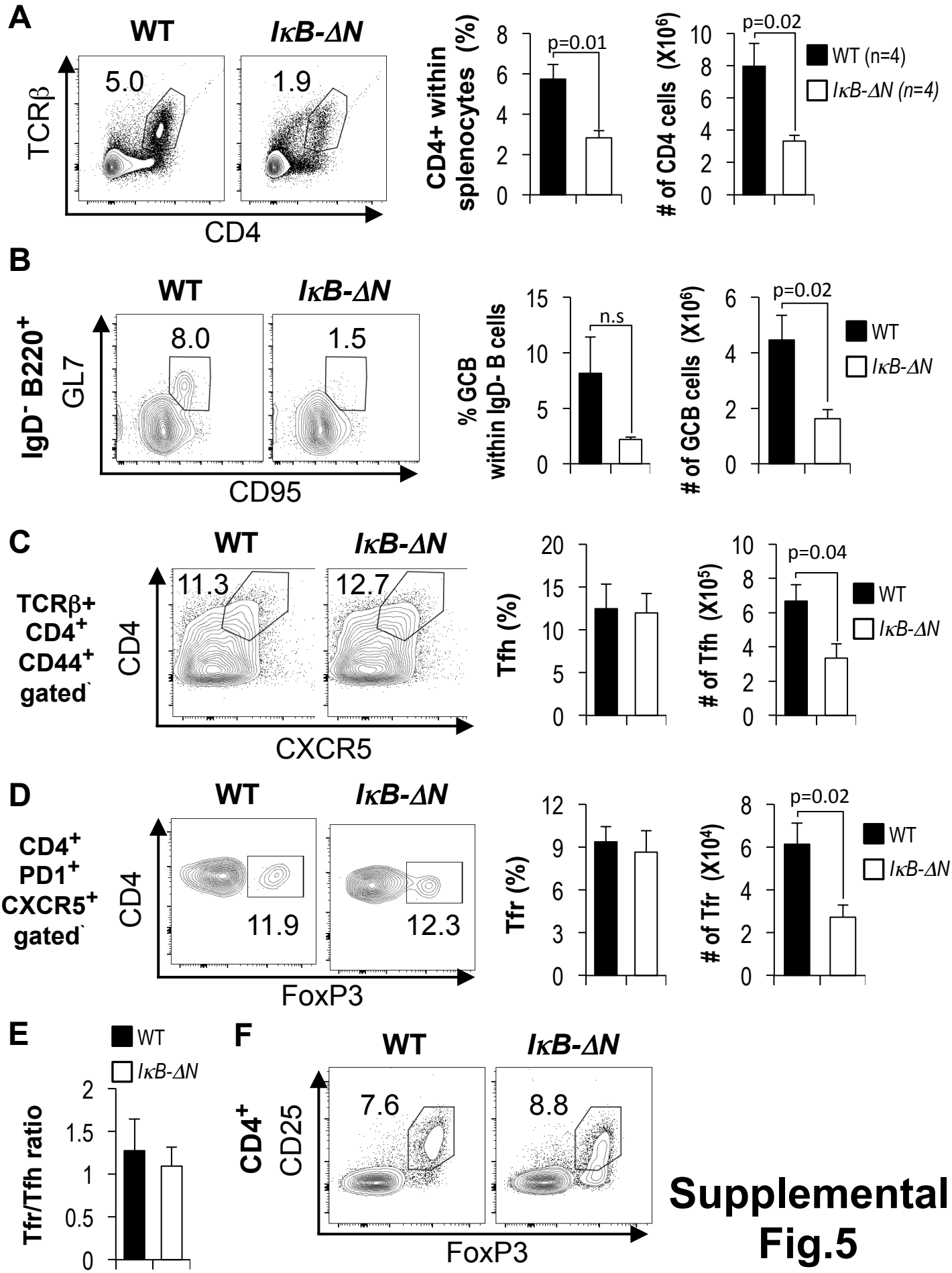

Supplemental Fig.5

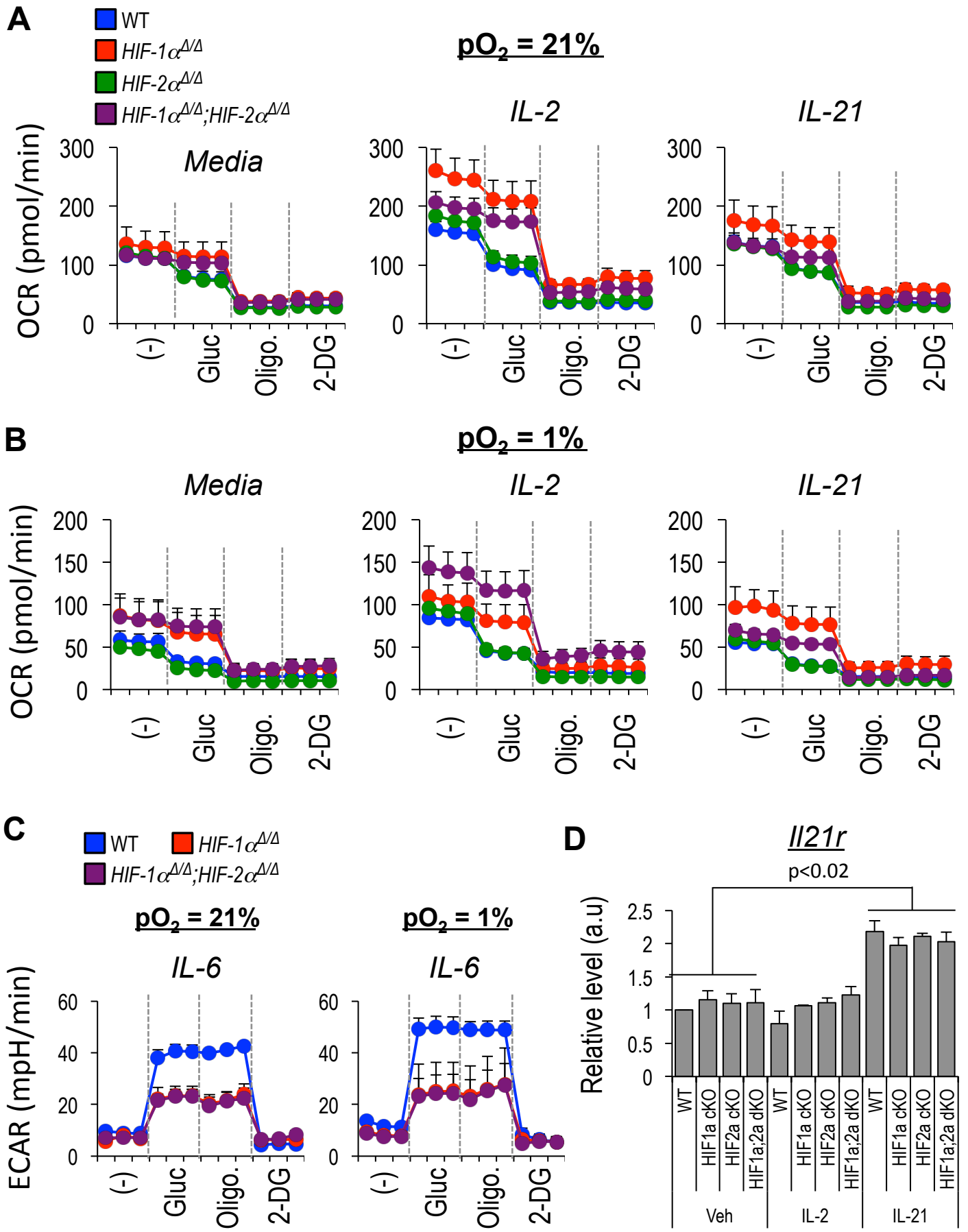

Supplemental Fig. 6

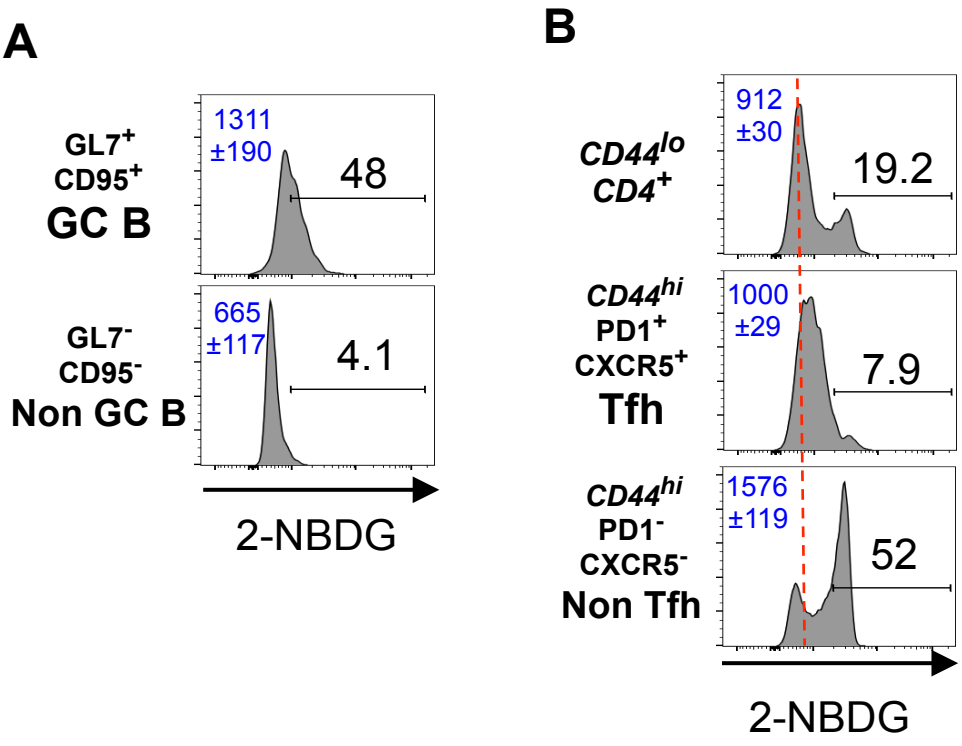

Supplemental Fig. 7

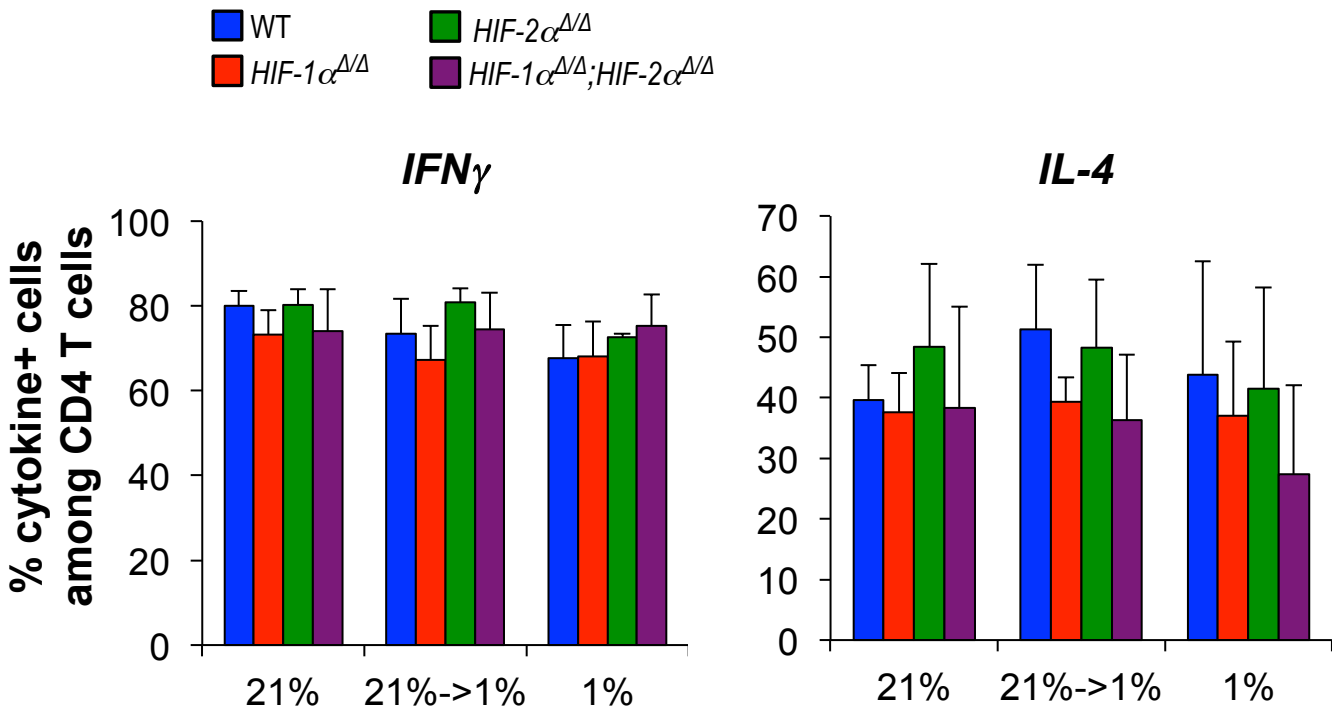

Supplemental Fig. 8

Supplemental Table 1. List of antibodies

Immunoblotting antibodies			
Antibody	**Supplier**	**Catalog #**	**Dilution Used**
HIF-1α Ab	Novus Biotech	NB100-449	1 : 1000
HIF-2α Ab	Novus Biotech	NB100-122	1 : 1000
Actin	Santa Cruz	sc-1616	1 : 2000
Donkey anti-Goat Alexa 680	Thermo	A-21084	1 : 5000
Goat anti-Rabbit Alexa 680	Thermo	A-21076	1 : 5000

Flow Cytometry Antibodies/ Immunofluorescence Antibodies			
Antibody	**Supplier**	**Catalog #**	**Dilution Used**
7-AAD	Life Technologies	A1310	1 : 1000
Ghost violetFluor450	Tonbo	13-0863	1 : 200
Fc Block (CD16/ CD32)	Tonbo	70-0161	1 : 50
CD4-APC	BD	553051	1 : 500
CD4-APCCy7	Tonbo	25-0042	1 : 500
PD1-PE	eBioscience	12-9985-81	1 : 250
CD44-FITC	BD	561859	1 : 500
CD44-APC	Tonbo	20-0441	1 : 500
FoxP3-eFluor660	eBioscience	50-5773-80	1 : 50
Bcl-6 APC	BD	561525	1 : 50
CXCR5-Biotin	BD	551960	1 : 200
TCRb-PerCPCy5.5	BD	553173	1 : 500
CD154-APC	eBioscience	17-1541-81	1 : 50
B220-FITC	Tonbo	35-0452	1 : 500
CD19-PECy7	Tonbo	60-0193	1 : 500
GL7-FITC	BD	562080	1 : 500
GL7-PE	BD	561530	1 : 500
IgM-FITC	BD	553437	1 : 500
IgG1-PE	BD	550083	1 : 500
IgD-PerCP Cy5.5	Biolegend	405709	1 : 500
Gr1-PerCPCy5.5	Tonbo	65-1276	1 : 500
CD11c-PerCPCy5.5	Tonbo	65-0114	1 : 500
CD11b-PerCPCy5.5	Tonbo	65-0112	1 : 500
F4/80-PerCPCy5.5	Tonbo	65-4801	1 : 500
CD95-Biotin	BD	554256	1 : 200
SA-PECy7	BD	557598	1 : 500
SA-APCCy7	BD	554063	1 : 500

ELISA/ ELISpot Antibodies			
Antibody	**Supplier**	**Catalog #**	**Dilution Used**
IgM-HRP	Southern Biotech	1010-05	1 : 2000
IgG1-HRP	Southern Biotech	1070-05	1 : 2000
IgG2c-HRP	Southern Biotech	1078-05	1 : 1000
IgG1-Biotin	Southern Biotech	1070-08	1 : 2000
IgG2c-Biotin	Southern Biotech	1078-08	1 : 1000

Supplemental Table 2. List of Primer pairs.

Primer Name	Sequence
Hif1a-F	5’-CAAGATCTCGGCGAAGCAA-3’
Hif1a-F	5’-GGTGAGCCTCATAACAGAAGCTTT-3’
Epas1-F	5’-CAACCTGCAGCCTCAGTGTATC-3’
Epas1-R	5’-CACCACGTCGTTCTTCTCGAT-3’
Il21-F	5’-GCCAAACTCAAGCCATCAAACC-3’
Il21-R	5’-TTCTCATACGAATCACAGGAAGGG-3’
Bcl6-F	5’-CTGCAGATGGAGCATGTTGT-3’
Bcl6-R	CACCCGGGAGTATTTCTCAG-3’
Prdm1-F	5’-GACGGGGGTACTTCTGTTCA-3’
Prdm1-R	5’-GGCATTATTGGGAACTGTGT-3’
Foxp3-F	5’-GGCCCTTCTCCAGGACAGA-3’
Foxp3-R	5’-GCTGATCATGGCTGGGTTGT-3’
Hprt-F	5’-TGAAGAGCTACTGTAATGATCAGTCAAC -3’
Hprt-R	5’-AGCAAGCTTGCAACCTTAACCA -3’